ACS OMEGA

http://pubs.acs.org/journal/acsodf

Article

Aggregation-Induced Emission-Based Material for Selective and Sensitive Recognition of Cyanide Anions in Solution and Biological Assays

Geeta A. Zalmi, Dinesh N. Nadimetla, Pooja Kotharkar, Avinash L. Puyad, Meenal Kowshik, and Sheshanath V. Bhosale*

Cite This: *ACS Omega* 2021, 6, 16704−16713

Read Online

ACCESS | Metrics & More | Article Recommendations | Supporting Information

ABSTRACT: Cyanide is one of the highly poisonous pollutants to our environment and toxic to human health. It is important to develop the widely applicable methods for their recognition to secure safe uses for people coming into contact and handling cyanide and their derivatives. In this regard, the aggregation-induced emission materials possess high potential for the development of simple, fast, and convenient methods for cyanide detection through either "turn-off" or "turn-on". Among the AIE-based materials, tetraphenylethylene is a promising sensor for various sensing applications. In this paper, we have designed and synthesized a TPE-based chemosensor, which shows high sensitivity and displays good selectivity for cyanide (CN^-) over others in the presence of interfering Cl^-, I^-, F^-, Br^-, HSO_4^-, $H_2PO_4^-$, NO_3^-, HCO_3^-, and ClO_4^- anions employed. The naked-eye, UV−vis, and fluorescence methods are employed to evaluate the performance of probe **1** toward CN^- detection. From these experiments, CN^- ions can be detected with a limit of detection as low as 67 nM, which is comparatively lower than that of the World Health Organization (WHO) permissible limit of the cyanide anion, that is, 1.9 μM. From the Job's plot, the 1:1 stoichiometric complexation reaction between probe **1** and CN^- was found. The probe was efficiently applied for the detection of CN^- ions using a paper strip method. The probe **1** also showed the potential of detecting CN^- ions in various food items and in the cell line.

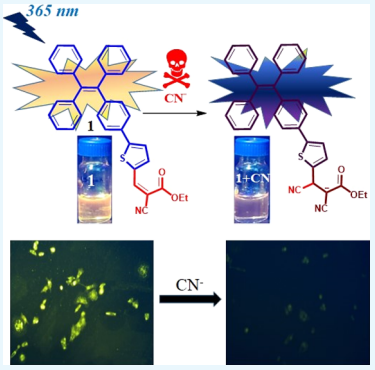

INTRODUCTION

Cyanide anions inhibit the mitochondrial electron transport in respiratory chain *via* binding with a ferric form of cytochrome P450.[1] The cyanide anions are the most toxic and cause serious damage to human health such as affecting the central nervous system and living environment.[2−5] Cyanide is extensively utilized in industrial factories particularly in gold mining, synthetic fiber, herbicides, and electroplating technology, and the presence of cyanide in environment and drinking water can cause a variety of diseases.[6−9] Furthermore, cyanide salts have been employed in the preparation of organic compounds and polymers, for example, nylon, nitrile rubber, acrylo nitrile-based polymer and acrylic plastics.[10] These human activities in the modern industry releases cyanide anions in the environment which ultimately enters the human body via drinking water and the food chain.[5,11,12] The World Health Organization (WHO) stipulates the permissible limit of cyanide anions in water to about 1.9 μM.[13] As a result of extreme toxic nature of cyanide anions in physiological and environmental systems, the efficient detection of cyanide (CN^-) ions is the need of the hour (instead of becoming very important for investigators).[14] Therefore, the development of an artificial probe with the potential of selectively recognizing and sensing CN^- ion species is being actively investigated.[15,16] The sensing methods are based on the formation of cyanide complexes with transition-metal ions,[17] the displacement method,[18] H-bonding interactions,[19,20] and luminescent approach.[21] However, these cyanide anion sensors exhibit some drawbacks such as poor selectivity in the presence of competing anions, for example, acetate and fluoride anions.[22] To overcome these drawbacks, nucleophilicity of CN^- ions has been utilized.[23] This method shows advantages of CN^- ion detection with high selectivity and sensitivity. This includes the nucleophilic reaction of CN^- ions with dibenzothiophene-based barbituric derivative,[24] carbazole-based sensor,[25] salicylaldehyde,[26] oxazine,[27] pyrylium,[28] acryltrizene,[29] acridinium,[30] squaranine,[31] trifluoroacetophenone,[32] imine,[33] and trifluoroacetamide[34] derivatives. Many researchers have developed optical methods/systems such as colorimetric and fluorescent probes for the detection of CN^- ions with the naked eye.[35−38]

Received: December 14, 2020
Accepted: March 19, 2021
Published: June 24, 2021

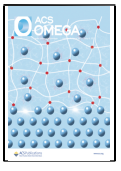

Scheme 1. Synthesis of Compound 1

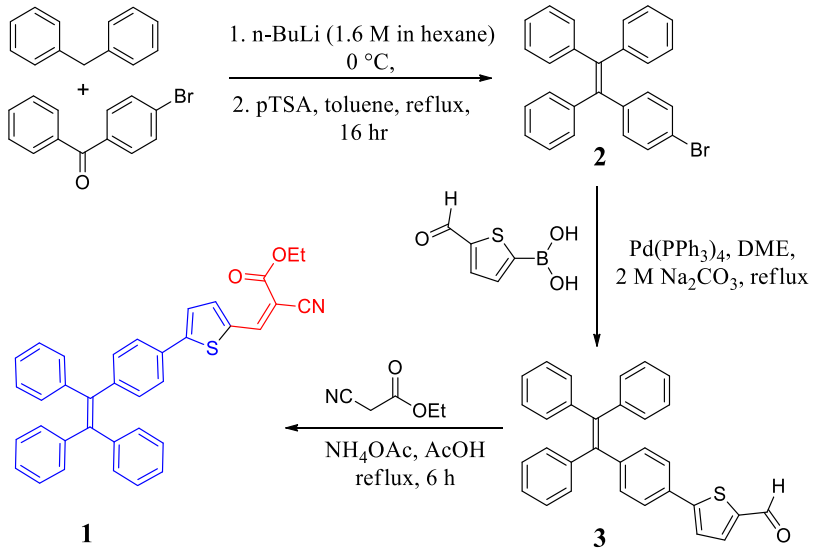

However, these molecules suffer from few drawbacks such as low sensitivity, tedious synthesis, being expensive, and naked-eye sensing. Therefore, it is still challenging to develop a sensor for the detection of CN^- ions with respect to the above-mentioned criteria.

In 2001, Tang et al. reported the new fluorescence phenomenon termed aggregation-induced emission (AIE).[39] They have demonstrated that the AIE probes emit no fluorescence in organic solutions, while it is significantly emissive in aqueous solutions via aggregate formation.[40] The AIE phenomenon results due to restriction of intramolecular motion in the aggregates. The sensing probes with AIE have attracted much attention for CN^- ion detection not only due to ease synthesis but also due to low cost and selectivity.[41−44]

In this manuscript, we report a simple and an efficient AIE active molecular architecture **1** (Scheme 1) for the detection of CN^- ions. Compound **1** showed high selectivity and sensitivity toward CN^- ions in tetrahydrofuran (THF)/H_2O (f_{water} = 99%). The results are monitored by employing naked eye, UV−vis, emission, and ^1H NMR changes. Furthermore, compound **1**-based paper strips under visible and UV light showed excellent and high sensitivity for CN^- ion detection. Moreover, it was employed successfully for CN^- ion detection in living cells with an obvious fluorescence change.

RESULTS AND DISCUSSION

Synthesis and Characterization of Compound *1*. Synthesis of the target molecule ethyl(*Z*)-2-cyano-3-(5-(4-(1,2,2-triphenylvinyl)phenyl)thiophen-2-yl)acrylate **1** was achieved *via* a multistep synthetic reaction strategy and is illustrated in Scheme 1. At the first stage, (2-(4-bromophenyl)-ethene-1,1,2-triyl)tribenzene (**2**) was easily prepared by condensing diphenylmethane and (4-bromophenyl) (phenyl)-methanone in the presence of *n*-BuLi followed by treating the intermediate with PTSA in dry toluene at reflux temperature. The yield of compound **2** was as high as 65%. The Suzuki coupling reaction between **2** and (5-formylthiophen-2-yl)-boronic acid resulted in the formation of 5-(4-(1,2,2-triphenylvinyl)phenyl)thiophene-2-carbaldehyde **3**. The target compound **1** was obtained by reacting compound **3** with ethyl 2-cyanoacetate *via* the Knoevenagel condensation reaction. The structure of compound **1** was confirmed by ^1H NMR, ^{13}C NMR, and elemental analysis (for the details, see the Supporting Information).

AIE Characteristics of Compound 1. After successful synthesis and characterization of compound **1**, we studied the mechanochromic properties by employing the process of grinding, fuming, and heating, as illustrated in Figure 1. The compound **1** in its solid powder form displays strong golden yellow fluorescence (quantum fluorescence yield Φ_F = 62.10) indicating AIE characteristics. We presume that the molecular packing in the solid state leads to exhibit strong emission properties due to restricted nonradiative relaxation pathways. However, it is observed that upon grinding, the color changes from golden yellow to bright yellow which is ascribed to the reduction in the crystalline size of the molecular architecture. Furthermore, on fuming the compound **1** with acetone, the grinded material could not revert to its original color intensity. However, when the compound **1** was heated, the luminescent properties were insignificantly changed from bright yellow to yellow. Thus, compound **1** exhibited significant mechanochromic characteristics with changes in fluorescence.

Thus, the solid powder of compound **1** exhibits strong golden yellow fluorescence. At first, we investigated the UV−vis and emission spectra of the probe in different solvents such as THF, acetonitrile (ACN), and dimethyl sulfoxide (DMSO). The results are depicted in Figure 2. The compound **1** shows absorption peaks at 410, 430, and 425 nm in THF, ACN, and DMSO (Figure 2a). Figure 2b shows that compound **1** displayed the fluorescence emission peaks at 565, 567, and 628 nm in THF, ACN, and DMSO solvents upon excitation at 410 nm, respectively. Herein, we observed that in THF, compound **1** shows very weak emission intensity as compared to ACN and DMSO. The UV−vis and emission spectral study indicates that the solvent plays an important role and attributed it as solvophobic effect.

The compound **1** is insoluble in aqueous media, however, displays good solubility in organic solvents, whereas its fluorescence in a pure organic solvent is weak. With the addition of water fraction from 0 to 99% in THF, compound **1** exhibits significant fluorescence in a THF/H_2O (f_w = 99%) solvent mixture under visible (Figure 3a) as well as UV light

https://doi.org/10.1021/acsomega.0c06080
ACS Omega 2021, 6, 16704−16713

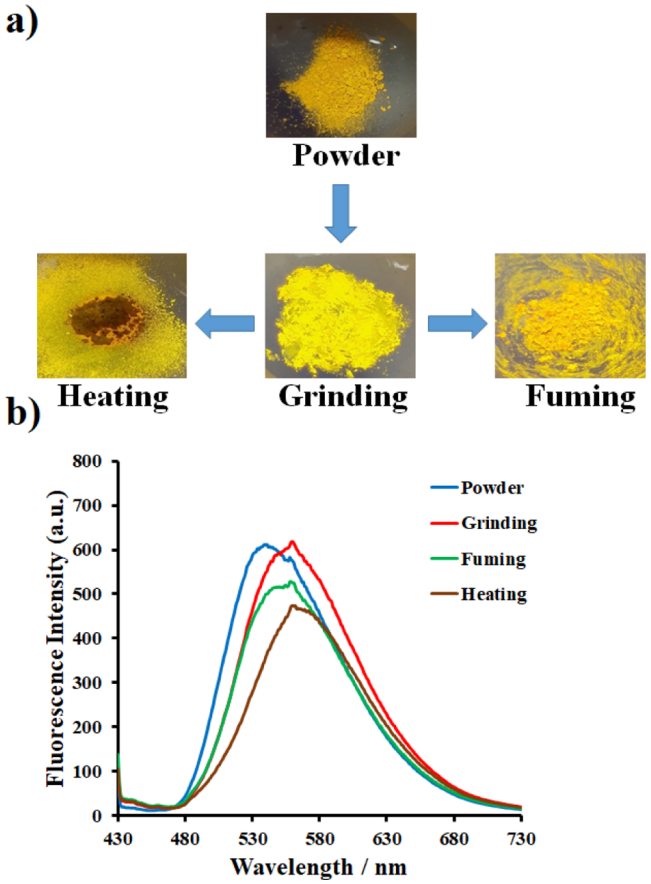

Figure 1. (a) Mechanochromic properties of probe **1** displaying the luminescence changing of it after grinding, fuming, and heating. (b) PL of powder, grinding, fuming, and heating of probe **1**.

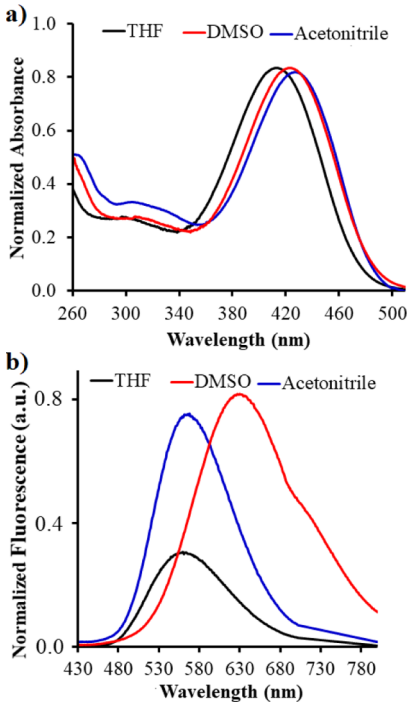

Figure 2. Normalized spectra of probe **1** in THF, acetonitrile, and DMSO solvents: (a) UV–vis and (b) fluorescence emission (λ_{ex} = 410 nm), respectively.

(Figure 3b). The change in emission properties suggests that the probe **1** clearly shows an AIE effect. The AIE characteristics of compound **1** were investigated using UV–vis absorption and fluorescence emission spectra in the THF/H_2O solvent mixture with different water fractions (f_w = 0 to 99%). UV–vis absorption spectra of compound **1** in THF and THF/H_2O are illustrated in Figure 3c. In THF, compound **1** exhibits the absorption maxima at 418 nm. Upon addition of 99% water, compound **1** showed the prominent absorption maxima at 426 nm with a red shift of 8 nm. This indicates that the addition of water leads to the formation of *J*-aggregation of compound **1**.

The corresponding fluorescence emission spectra are illustrated in Figure 3d. Upon excitation at λ_{ex} = 410 nm, compound **1** showed very weak emission spectra in THF solution at 565 nm (Figure 3d, green line). Upon incremental addition of water (f_w = 20, 40, and 60%), the fluorescence intensity slightly decreased with a red shift may be due to small particular aggregates. A slight increase in emission intensity was observed at f_w = 80%. At 99% of water fraction in THF solution of compound **1**, a significant fluorescence intensity enhancement was observed (Figure 3d, red line). Thus, the fluorescence quantum yields of compound **1** increased from 1.3% in THF to 7.8% in THF/H_2O solvent mixtures with 99% of water fraction. The change in emission intensity with % of water in THF is illustrated in Figure 3d. These results indicated that the compound **1** possessed excellent AIE characteristics and exhibited the highest fluorescence intensity in THF/H_2O (f_w = 99%).

Sensing Performance of Probe 1. To the solution of 2 × 10^{-5} M compound **1** (coded as: "probe **1**" onward) in DMSO, a series of anions in its tetrabutylammonium salts of CN^-, Cl^-, I^-, F^-, Br^-, HSO_4^-, $H_2PO_4^-$, NO_3^-, HCO_3^-, and ClO_4^- (8 × 10^{-5} M) were added. The changes in color under day light and UV–vis (365 nm) light were monitored and illustrated in Figure 4a,b, respectively. Under day light, probe **1** in DMSO displayed yellow fluorescence color (Figure 4a). With the addition of anions, we observed that except CN^- ions, the solutions with the test anions showed yellow color. While the probe **1** solution in DMSO with only CN^- ions exhibited red fluoroscent color. As shown in Figure 4b, under UV–vis light at 365 nm, the solutions of probe **1** (buff in color) with the addition of different anions showed buff color, whereas in the presence of CN^- ions displayed wine red color. These results indicate that the compound **1** detected CN^- ions with good selectivity. Thus, probe **1** can be utilized as a naked-eye colorimetric and fluorescent sensor for CN^- ions.

UV–Vis Absorption Study. The UV–vis absorption spectra of probe **1** and with the addition of each anion were studied and are illustrated in Figure 5a. Probe **1** in DMSO (2 × 10^{-5} M) exhibited absorption maxima at 425 nm. The UV–vis absorption of probe **1** with the addition of each tested anion (8 × 10^{-5} M) displayed almost no significant change except for CN^- ion addition. The addition of CN^- ions showed pronounced changes in the absorption spectra, the absorption maxima at 425 were completely disappeared and a new band appeared at 345 nm with the shoulder peak at 302 nm. The UV–vis absorption changes might be due to the nucleophilic addition of CN^- ions to probe **1**. This may cause interruption of intramolecular charge transfer (ICT) effect which ultimately led to affect the optical and photophysical characteristics. Thus, probe **1** can be utilized for the detection of CN^- ions with high selectivity. To get detail insight, we titrated probe **1**

https://doi.org/10.1021/acsomega.0c06080
ACS Omega 2021, 6, 16704–16713

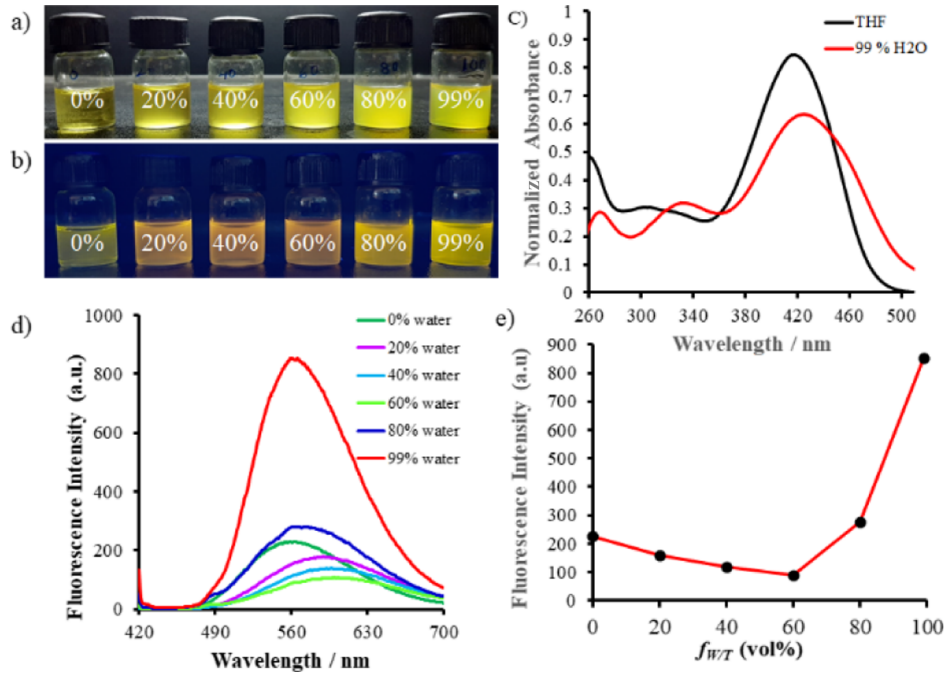

Figure 3. Photograph of compound **1** (2×10^{-5} M) in THF/H_2O mixtures with different f_w (0–99%) under (a) visible light and (b) 365 nm UV light; (c) UV–vis absorption spectra in THF and THF/H_2O f_w (0 to 99%). (d) Fluorescence emission spectra of the compound **1** in THF/H_2O (v/v) mixtures with different water fractions at λ_{ex} = 410 nm and (e) plot of relative fluorescence emission intensity as a function of f_w.

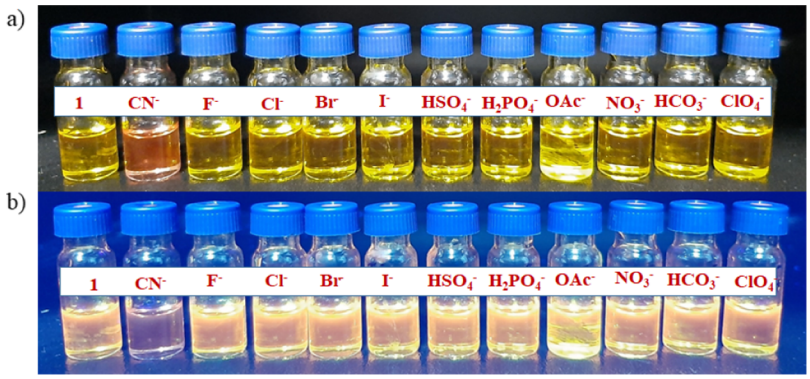

Figure 4. Solutions of probe **1** in DMSO; probe **1** is without any anions and respective with the addition of 4 equiv of tetrabutylammonium salts of CN^-, Cl^-, I^-, F^-, Br^-, HSO_4^-, $H_2PO_4^-$, NO_3^-, HCO_3^-, and ClO_4^- with probe **1**: (a) under visible light (naked eye) and (b) under UV light 365 nm, respectively.

with CN^- ions in DMSO and the results are depicted in Figure 5b. The UV–vis absorption changes were monitored with the incremental addition of CN^- (0 to 8×10^{-5} M) ions to probe **1** in DMSO. We observed that with the increase in amount of CN^- ions in probe **1**, the absorption maxima at 425 nm gradually decreased and completely disappeared at 4 equiv of CN^- ions. At the same time, new absorption maxima at 345 nm appeared with increasing intensity along with a shoulder peak at 302 nm. Herein, one isosbestic point at 365 nm also appeared. These UV–vis absorption spectral changes are attributed to a nucleophilic addition reaction between probe **1** and CN^- ions resulting in the molecular structure changes.

Fluorescence Emission Study. A fluorescence emission spectral study was performed to investigate the detection performance of probe **1** toward CN^- ions in DMSO. The obtained results are illustrated in Figure 6a,b. As shown in Figure 6a, the probe **1** in DMSO upon excitation at 410 nm exhibited the fluorescence emission band at 628 nm. With the addition of series of anions, tetrabutylammonium salts of CN^-, Cl^-, I^-, F^-, Br^-, HSO_4^-, $H_2PO_4^-$, NO_3^-, HCO_3^-, and ClO_4^- (8×10^{-5} M), the changes in the emission band at 628 nm were monitored. The fluorescence spectra (628 nm) of probe **1** did not display significant changes even with the addition of 4 equiv of each tested anion except for CN^- ions. It was observed that in the presence of CN^- ions, the emission intensity of probe **1** at 628 nm completely disappeared. This is attributed to the breaking of ICT of probe **1**. Fluorescence titration experiments were performed to investigate the sensing ability of probe **1** with the incremental addition of CN^- ions (0–8×10^{-5} M). The changes in fluorescence emission spectra were recorded and are depicted in Figure 6b. As illustrated in Figure 6b, with the incremental addition of CN^- ion to probe **1**, the fluorescence emission band at 628 nm gradually decreased and finally disappeared.

Subsequently, the quantum yield of the probe **1** (Φ) was estimated and found to be 6.3 in DMSO at room temperature.

https://doi.org/10.1021/acsomega.0c06080
ACS Omega 2021, 6, 16704–16713

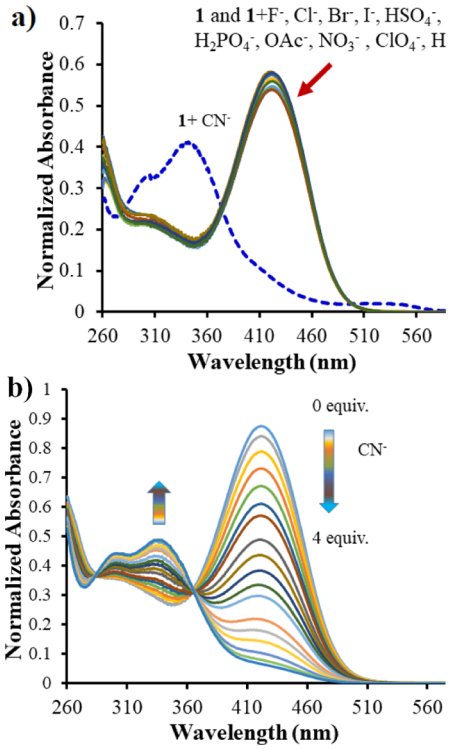

Figure 5. UV−vis absorption spectra of probe **1** (2×10^{-5} M) in the presence of (a) 4 equiv of Cl^-, I^-, F^-, Br^-, HSO_4^-, $H_2PO_4^-$, NO_3^-, HCO_3^-, and ClO_4^- (8×10^{-5} M) as tetrabutylammonium salts and CN^- ions as a tetraethylammonium salt. (b) Addition of the tetraethylammonium salt of CN^- (0 to 8×10^{-5} M) in DMSO.

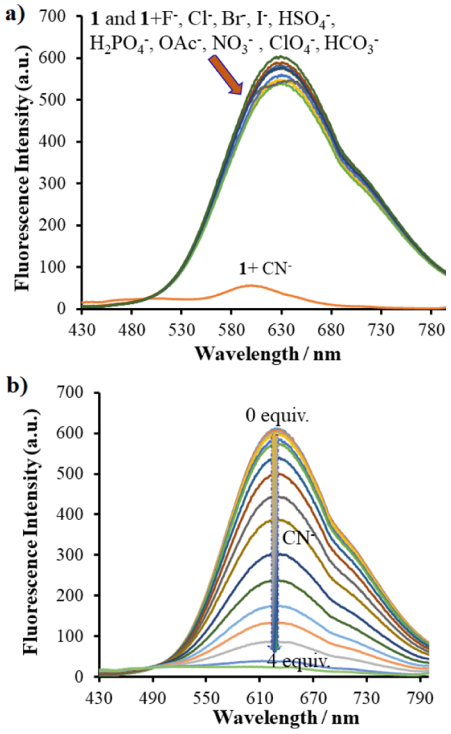

Figure 6. Emission spectra of probe **1** (2×10^{-5} M) in the presence of (a) 4 equiv of Cl^-, I^-, F^-, Br^-, HSO_4^-, $H_2PO_4^-$, NO_3^-, HCO_3^-, and ClO_4^- (8×10^{-5} M) as tetrabutylammonium salts and CN^- ions as a tetraethylammonium salt. (b) Addition of the tetraethylammonium salt of CN^- (0 to 8×10^{-5} M) in DMSO.

As shown in Figure 6b, the fluorescence intensity gradually decreased and disappeared with the addition of CN^- ions (4 equiv) and the quantum yield of the **1**:CN^- decreased to 0.09. This fluorescence emission behavior is attributed to the selective detection of CN^- ions.

Stoichiometry Analysis and Binding Constant. In order to determine the binding mode between probe **1** and CN^- ion, the Job's plot and Benesi−Hildebrand plot[45] were analyzed and are illustrated in ESI, Figure S1. The plot of changes in fluorescence emission intensity against the molecular fraction of [**1**]/[**1**+CN^-] is illustrated in Figure S1a. Job's plot results clearly indicate a 1:1 stoichiometric complexation reaction between probe **1** and CN^-. The Benesi−Hildebrand plot (Figure S1b) was employed to determine the binding constant (K) between probe **1** and CN^- ions. The linear relationship of fluorescence emission intensity as a function of [CN^-] from 0 to 4 equiv (R = 0.9831) was found graphically. The binding constant (K_a) of **1** with CN^- was found to be 4.78×10^6 M^{-1}.

Limit of Detection. The calculated limit of detection (LOD = $3\sigma/S$), where σ is the standard deviation of the blank sample and S is the absolute value of the slope between fluorescence emission intensity and concentration of CN^- of the probe **1** is 67 nM, which is very low as compared to the maximum permissible level of CN^-, according to the WHO (1.9 mM) agency guide lines (Figure S2, Table S2). This suggests that the probe **1** could be employed as a sensitive fluorescent probe for the quantitative detection of CN^- at nanomolar levels.

Competitive CN^- Ion Binding. In order to explore the specificity of the probe **1** as an anion-selective fluorescence sensor for CN^- ions, competitive experiments of probe **1** were carried out by utilizing various anions (4 equiv) as the interfering anions. As depicted in Figure S3, the blue bar corresponds to the probe **1** with the tested anions (F^-, Cl^-, Br^-, I^-, HSO_4^-, $H_2PO_4^-$, OAc^-, NO_3^-, ClO_4^-, and HCO_3^-), whereas the red bar corresponds to the probe **1** with one of the tested anions in the presence of CN^- ions. It was observed that CN^- could clearly diminish the fluorescence of probe **1** in the presence of other anions. The abovementioned results strongly suggest that the tested anions has no effect on probe **1** for CN^- ion detection. Thus, probe **1** could be employed as a fluorescence sensor for CN^- ion recognition with outstanding selectivity and good anti-interference.

CN^- Detection Mechanism by ^{1}H NMR Spectra of 1 and 1 in the Presence of CN^-. To confirm the binding mechanism of the CN^- ion with the probe **1**, ^{1}H NMR experiments were performed in DMSO-d_6 and are illustrated in Figure 7. Probe **1** exhibits a characteristic peak at δ 8.55 ppm, attributed to the vinylidene proton "H_1" (Figure 7a). Upon addition of TEACN (1.2 equiv) to the probe **1**, the peak at 8.55 ppm in ^{1}H NMR completely disappeared, while the new peak at 5.09 ppm was observed. This peak was assigned to H_2 (Figure 7b). Subsequently, thiophene proton peaks move significantly to higher frequencies. This leads to alteration in the original molecular architecture of probe **1**. These results indicate that CN^- ions with strong nucleophilicity attacked the vinylidene C=C bond and break the ICT between electron donor TPE and the electron acceptor functional group of the probe **1**.

Theoretical Calculations. To further investigate the sensing properties of **1** toward the CN^- ion detection mechanism and photophysical characteristic changes, density

https://doi.org/10.1021/acsomega.0c06080
ACS Omega 2021, 6, 16704−16713

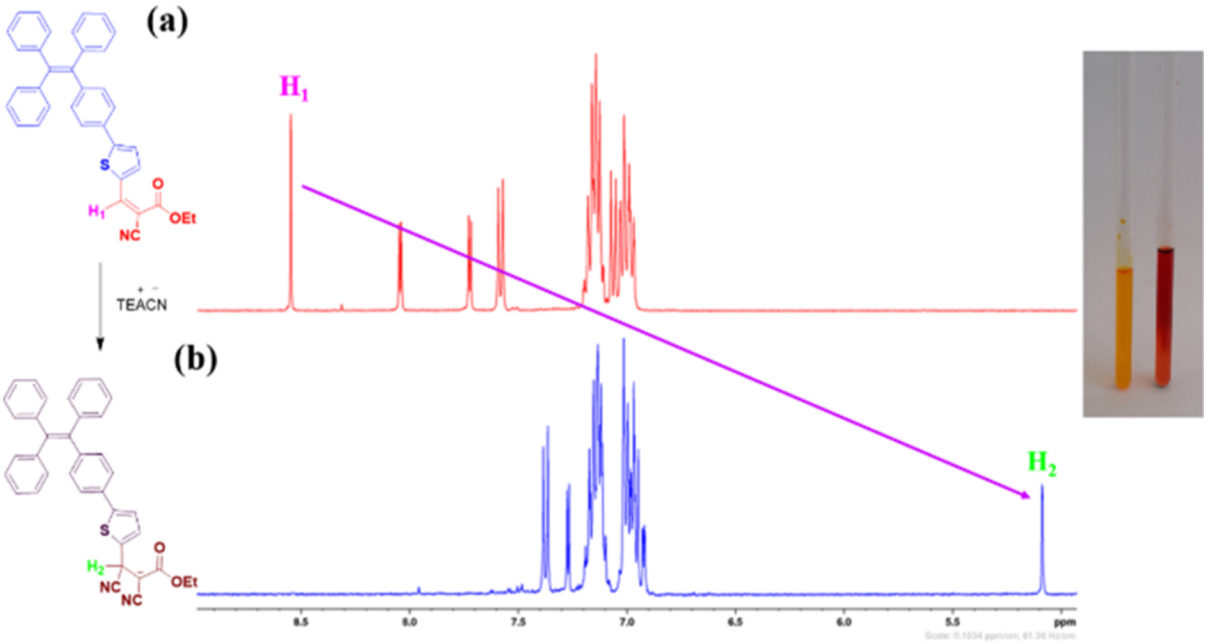

Figure 7. ^{1}H NMR spectral changes of probe **1**: in DMSO-d_6 (a) and upon the addition of 1.2 equiv CN^- anions (b).

functional theory (DFT) and time-dependent DFT (TD-DFT) calculations were performed. The results of the calculations carried out have been obtained using the Gaussian 09 *ab initio*/DFT quantum chemical simulation package.[46] The geometry optimization of molecules in the series **1** and **1**-CN^- was carried out at the B3LYP/6-31G* level of theory. In order to confirm the minima, frequency calculations also have been carried out at the same level. The frontier molecular orbitals (FMOs) of **1** and **1**-CN^- are generated using Avogadro[47,48] and are illustrated in Figures 8 and S4. The highest occupied molecular orbital (HOMO) of probe **1** was mainly delocalized on the tetraphenylethylene (TPE) moiety and thiophene ring system, whereas the lowest unoccupied molecular orbital (LUMO) was distributed over the phenyl ring of TPE, thiophene subunit, and nitrile functional group. In contrast, the HOMO of **1**-CN^- was located on the ethylcyanoacetate subunit along with the new CN^- moiety, while the LUMO was mainly delocalized over the TPE and thiophene ring system. These results suggested that the introduction of the CN^- subunit had an impact on the charge transition properties of the probe **1**. The DFT calculations were in agreement with the experimental results, which suggested that the nucleophilic addition reaction of CN^- ions and probe **1** takes place by reacting with the C═C bond. This resulted in the inhibition of the ICT effect of **1** with the addition of CN^-. Furthermore, the geometries of probe **1** and **1**:CN^- obtained at the B3LYP/6-31G* level were subjected to TD-DFT studies using the B3LYP/6-31G* level for charge-transfer excitations. TD-DFT results were analyzed by employing Gauss-Sum 2.2.5 program,[49] TD-DFT results obtained are reported in Table S1, it shows LUMO density toward cyanide, which is already discussed in the literature.[56] From the TD-DFT results, it is seen that probe **1** (Figure S5) has absorption with high intensity compared with **1**:CN^- (Figure S6). Calculation of the HOMO and LUMO from CV is shown in Table S3.

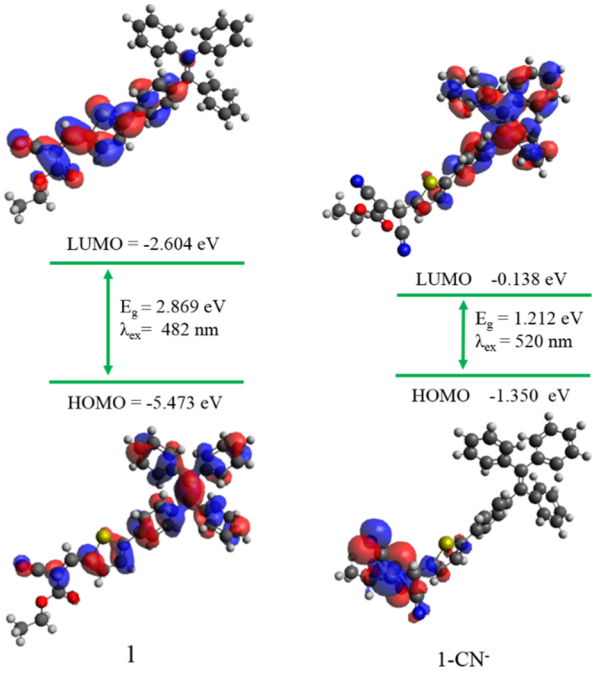

Figure 8. Optimized geometric structures of **1** and **1**:CN^- are shown.

Test Strip for CN^- Detection Using Probe 1. To employ the probe **1** for practical purpose, we prepared the test strip using chloroform solution and examined the detection of CN^-. The results are depicted in Figure S7a,b. The test paper of probe **1** is in yellow color. It was found that in sunlight, the paper strip test paper of **1** changed its color from yellow to colorless after CN^- addition (Figure S7a), whereas other anions do not display any impact. Moreover, we also investigated the color change on strip **1** under 365 nm UV light. It was observed that fluorescence of the probe **1** changed from dark yellow to colorless (Figure S7b).

Application of Probe 1 in Food Samples. Furthermore, to investigate the application of probe **1** in food analysis, we selected food samples containing cyanogenic glycosides including bitter almonds, sweet potato, and sprouting potato

https://doi.org/10.1021/acsomega.0c06080
ACS Omega 2021, 6, 16704−16713

to check the utility of probe **1** to check the endogenous cyanide.[50,51] The food samples were prepared by crushing and pulverizing 10 g of food samples using mortar and pestle. After that, 10 mL of water was added followed by the addition of 5 mg of NaOH under constant stirring for 10 min and then the mixture was centrifuged for 20 min and the mixture of cyanide-containing solution was obtained.[52,53] Upon the addition of cyanide-containing solution to the probe, the fluorescence completely disappears, as shown in Figure 9. Therefore, the

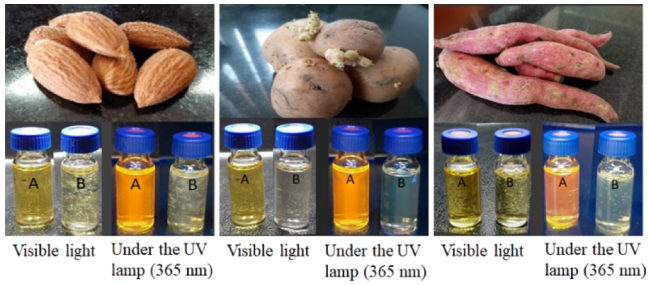

Figure 9. Vial "A" contains stock solution of probe **1** in DMSO, and vial "B" contains stock solution of probe **1** plus the respective food sample. Images are taken separately and included together in the single figure.

probe **1** could be effectively and potentially used for detecting cyanide in cyanogenic glycoside-containing food samples. The details are as follows: a solution of probe **1** in DMSO was taken in 5 different test vials. To each vial, probe **1**, water **2**, NaOH **3**, food extract **4**, and TEACN$^-$ **5** were added, respectively. It was observed that under UV−vis light illumination at 365 nm, there was a significant change in fluorescence, wherein complete quenching of fluorescence takes place upon the addition of TEACN and food extract (Figure S9).

Application of Probe 1 in Living Cells. *Cell Cytotoxicity.* HeLa cells were stable until a concentration of 30 nM, however, 10 nM showed a percentage viability of 100% even after 24 h of incubation with probe **1**. This shows that 10 nM concentration of probe **1** is not cytotoxic to HeLa cells and hence the same was used for fluorescence uptake studies (for details, see experimental Figure S8).

Cell Imaging. Figure 10a,b shows the HeLa cells under bright field and FITC fluorescence filter, respectively. When the HeLa cells were incubated with 10 nM of the probe **1** and observed under bright field (Figure 10c) and FITC fluorescence filters, the green fluorescence observed (Figure 10d) clearly shows that probe **1** is taken up by the cells and the cells remain viable. Upon the addition of CN$^-$, the presence of cells was confirmed in the bright-field image (Figure 10e), however, no fluorescence was seen under the FITC filter, clearly indicating the fluorescence quenching of probe **1** in HeLa cells, due to the reaction between intracellular cyanide and probe **1** (Figure 10f). Thus, these results indicate that the probe **1** penetrates through the HeLa cells and detects the CN$^-$. We believe that in future, probe **1** and similar AIE-active compounds could find potential applications as *in vivo* fluorescence sensors for the detection of CN$^-$ in live cells.

Table S2 shows the comparison of probe **1** with small organic molecules used for cyanide sensing in the literature. Inspite of the literature study of organic molecules used for selective cyanide sensing with good LOD's, however, they suffer drawbacks of either lack of test strip, cell imaging, or AIE

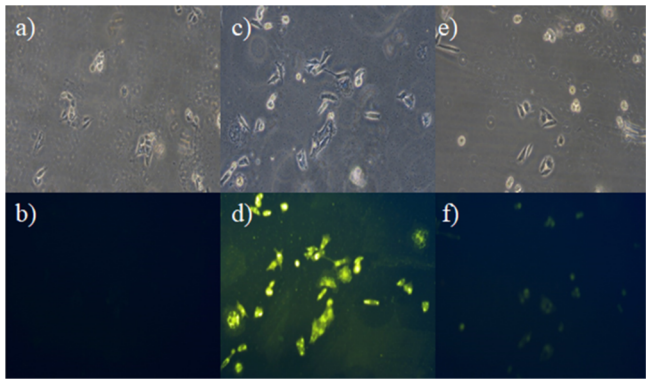

Figure 10. (a) HeLa cells in bright field, (b) no auto fluorescence observed in HeLa cells using an FITC filter, (c) HeLa cells incubated with probe **1** in bright field, (d) HeLa cells with probe **1** exhibiting green fluorescence, (e) HeLa cells with probe **1** and CN in bright field, and (f) HeLa cells with probe **1** and CN in green fluorescence.

activity.[54,55] Thus, our probe **1** is shown to be superior as compared with the literature probe, as it produces very good LOD along with naked eye detection, colorimetric fluorescence, and test strip as well as cell imaging.

CONCLUSIONS

In summary, we have successfully synthesized a probe **1** and employed for sensing of anions. Probe **1** shows naked eye colorimetric and fluorescent sensing of CN$^-$ (tetraethylammonium salt) selectively over other anions such as Cl$^-$, I$^-$, F$^-$, Br$^-$, HSO_4^-, $H_2PO_4^-$, NO_3^-, HCO_3^-, and ClO_4^- (as a tetrabutylammonium salt) used in this study in a DMSO solvent. The selectivity and sensitivity for CN$^-$ ions with probe **1** are found to be very high. The probe **1** exhibited very low LOD, that is, 67 nM. Furthermore, a paper strip was developed to display the CN$^-$ sensing and also probe **1** was employed for the detection of CN$^-$ ions from various food components. Furthermore, probe 1 was also used to detect CN$^-$ ions in living cells, which clearly suggested that the probe **1** could be a good sensor for practical applications.

EXPERIMENTAL SECTION

Chemicals and Reagents. Compounds **2** and **3** were obtained through the procedure mentioned in the literature,[54] and probe **1** was synthesized by reacting ethyl cyanoacetate and 5-(4-(1,2,2-triphenylvinyl)phenyl)thiophene-2-carbaldehyde **3**, in the presence of ammonium acetate and acetic acid as a solvent. Various anions of tetrabutylammonium salts (Cl$^-$, I$^-$, F$^-$, Br$^-$, HSO_4^-, $H_2PO_4^-$, HCO_3^-, NO_3^-, and ClO_4^-) and tetraethylammonium cyanide (CN$^-$) salt and DMSO were purchased from Sigma-Aldrich and TCI. ^{1}H NMR spectra were recorded on 400 MHz and ^{13}C NMR using a 100 MHz Bruker spectrometer. Tetramethylsilane (TMS) was used as an internal standard. The $CDCl_3$-*d* and DMSO-d_6 were used as a deuterated solvent. Mass spectrometric data were obtained using a positive electron spray ionization (ESI-MS) technique on an Agilent Technologies 1100 Series (Agilent Chemistation Software) mass spectrometer. UV−vis absorption spectra were recorded using a UV−vis-1800 Shimadzu spectrophotometer and fluorescence emission was measured on an Agilent, Carry Eclipse spectrofluorophotometer.

UV−Vis and Fluorescence Experiments. *UV−Vis and Fluorescence of the Probe 1 upon the Addition of 4 equiv*

https://doi.org/10.1021/acsomega.0c06080
ACS Omega 2021, 6, 16704−16713

Anions. The 2 mL probe **1** (2×10^{-5} mol/L) in DMSO was placed in solution in the quartz cell, and the absorption and fluorescence spectra were recorded. Different anions (8×10^{-5} M) were added as salts such as $TBANO_3$, TBAF, TBACN, $TBAH_2PO_4$, TBACl, TBABr, $TBAHCO_3$, TBAI, $TBAHSO_4$, and TEACN, and the absorption and fluorescence spectra were recorded at room temperature.

UV−Vis and Fluorescence Titration of the Probe 1 upon the Addition of CN^- Anions. The 2 mL probe **1** (2×10^{-5} mol/L) in DMSO was placed in solution in the quartz cell and fraction of TEACN ($0-8 \times 10^{-5}$ M) ion solution was added, and the corresponding absorption and fluorescence spectra of the probe were recorded at room temperature.

Naked-Eye Detection. The stock solution of the probe **1** was prepared by (2×10^{-5} mol/L) dissolving it in DMSO solvent. The various anions of salt forms such as $TBANO_3$, TBAF, TBACN, $TBAH_2PO_4$, TBACl, TBABr, $TBAHCO_3$, TBAI, $TBAHSO_4$, and TEACN dissolved in DMSO (2×10^{-3} M) were added, and the pictures were taken under visible light and UV light 365 nm.

Paper Strip Preparation. Test strips were prepared and immersed in the solution of the probe in chloroform. The strips were air-dried. These test strips were used for detecting cyanide in the presence of other anions. The test strips were observed under a UV lamp and used for easy naked-eye detection.

Sensing of Cyanide in Food Samples. A solution of probe **1** (0.5 mL) in DMSO was taken in a test vial, and second, vial probe **1** (0.5 mL) and food extract were added (see details in the Results and Discussion section), respectively. It was observed that under UV−vis light illumination at 365 nm, there was significant change in fluorescence, wherein complete quenching of fluorescence takes place upon the addition of food extract.

Cell Toxicity of Probe 1. For determining the cytotoxicity of probe **1**, HeLa cells were initially grown in culture media comprising Dulbecco's modified Eagle's medium (DMEM) supplemented with 5% fetal bovine serum. The exponentially growing cells were then seeded at a density of 5×10^4 cells per well in a 96-well plate and incubated for 24 h in an environment with 5% CO_2 at 37 °C temperature. Subsequently, probe **1** was added to the wells at concentrations ranging from 10 to 100 nM and incubated for 24 h. The cells were given a PBS wash and 0.5 mg/mL of MTT solution prepared in DMEM was added to the wells and incubated for 4 h. The obtained formazan crystals were dissolved in DMSO and the concentration of formazan crystals was measured using a multiwell spectrophotometer (Schimadzu Multiskan Go) using untreated cells as the control. All the experiments were carried out in triplicates.

Cell Imaging. For the detection of cyanide in a biological system, HeLa cells were used to check the uptake of probe **1**. HeLa cells were seeded on sterile cover slips in 12-well plates at a density of 5×10^4 cells per well and incubated at 37 °C for 24 h with 5% CO_2 in a CO_2 incubator (Thermoscientific). The cells were then incubated with 10 nM conc. of probe **1** for 60 min and imaged using an epifluorescence microscope (Olympus Inverted Trinocular Microscope). Furthermore, to check whether the fluorescence is affected by quenchers such as cyanide, the cells treated with probe **1** were again incubated with cyanide for 30 min and the fluorescence was observed under an epifluorescence microscope.

■ ASSOCIATED CONTENT

Supporting Information

The Supporting Information is available free of charge at https://pubs.acs.org/doi/10.1021/acsomega.0c06080.

Binding constant, Job plot, DFT calculations, comparative table, strip test, and characterization of molecules (PDF)

■ AUTHOR INFORMATION

Corresponding Author

Sheshanath V. Bhosale − *School of Chemical Sciences, Goa University, Taleigao Plateau, Goa 403206, India;* orcid.org/0000-0003-0979-8250; Email: svbhosale@unigoa.ac.in

Authors

Geeta A. Zalmi − *School of Chemical Sciences, Goa University, Taleigao Plateau, Goa 403206, India*

Dinesh N. Nadimetla − *School of Chemical Sciences, Goa University, Taleigao Plateau, Goa 403206, India*

Pooja Kotharkar − *Department of Biological Sciences, BITS Pilani, Zuarinagar, Goa 403726, India*

Avinash L. Puyad − *School of Chemical Sciences, Swami Ramanand Teerth Marathwada University, Nanded, Maharashtra 431606, India*

Meenal Kowshik − *Department of Biological Sciences, BITS Pilani, Zuarinagar, Goa 403726, India;* orcid.org/0000-0002-7308-5207

Complete contact information is available at: https://pubs.acs.org/10.1021/acsomega.0c06080

Author Contributions

G.A.Z. and D.N.N. contributed equally. The manuscript was written through contributions of all authors. All authors have given approval to the final version of the manuscript.

Notes

The authors declare no competing financial interest.

■ ACKNOWLEDGMENTS

S.V.B. (GU) acknowledges University Grant Commission (UGC) Faculty Research Program, New Delhi, India [F.4-5(50-FRP) (IV-Cycle)/2017(BSR)], for an award of Professorship and also acknowledges Council of Scientific & Industrial Research (CSIR), New Delhi, code no. 02(0357)/19/EMR-II and DST-Goa for providing financial support under project no. GEC/ppl/Govt.dept/41/14/314. D.N.N. acknowledges CSIR-UGC for Senior Research Fellowship (SRF).

■ DEDICATION

$^{\perp}$G.A.Z. dedicates this work to her lovely parents on the occasion of their birthday's i.e. 55th of her father Anant S. Zalmi and 50th of her mother Anandi A. Zalmi.

■ REFERENCES

(1) Vennesland, B.; Comm, E. E.; Knownles, C. J.; Westly, J.; Wissing, F. *Cyanide in Biology*; Academic: London, 1981.

(2) Kuling, K. W. *Cyanide Toxicity*; U.S. Department of Health and Human Services: Atlanta, GA, 1991.

(3) Kuling, K. W.; Ballantyne, B. *Cyanide Ttoxicity*. U. S. Department of Health & Human Services, Public Health Services, Agency for Toxic Substances and Disease Registry, 1991.

(4) Gerberding, J. L. *Toxicology Profile for Cyanide*; U. S. Department of Health and Human Services: Atlanta, 2006.
(5) Bianchi, A.; Bowman-James, K.; Garcia-Espana, E. *Supramolecular Chemistry of Anions*; Wiley-VCH: New York, NY, USA, 1997.
(6) Zhou, X.; Mu, W.; Lv, X.; Liu, D. Ratiometric fluorescent detection of CN- based on CN- promoted interruption of π-conjugation of a coumarin-bearing Michael receptor. *RSC Adv.* **2013**, *3*, 22150−22154.
(7) Chen, C.-L.; Chen, Y.-H.; Chen, C.-Y.; Sun, S.-S. Dipyrrole carboxamide derived selective ratiometric probes for cyanide ion. *Org. Lett.* **2006**, *8*, 5053−5056.
(8) Nicoleti, C. R.; Nandi, L. G.; Machado, V. G. Chromogenic chemodosimeter for highly selective detection of cyanide in water and blood plasma based on Si-O cleavage in the micellar system. *Anal. Chem.* **2015**, *87*, 362−366.
(9) Miller, G. C.; Pritsos, C. A. *Cyanide: Soc., Ind. Econ. Aspects, Proc. Symp. Annu. Meet. TMS* **2001**, *73*, 81.
(10) *Ullmann's Encyclopedia of Industrial Chemistry*, 6th ed.; Wiley-VCH: New York, 1999.
(11) Young, C.; Tidwell, L.; Anderson, C. *Cyanide: Social, Industrial, and Economic Aspects*; Minerals, Metals, and Materials Society: Warrendale, 2001.
(12) Bolarinwa, I. F.; Orfila, C.; Morgan, M. R. A. Determination of amygdalin in apple seeds, fresh apples and processed apple juices. *Food Chem.* **2015**, *170*, 437−442.
(13) Organisation mondiale de la santé, World Health Organization, World Health Organisation Staff. *Guidelines for Drinking-Water Quality*; World Health Organization: Geneva, Switzerland, 1996.
(14) Xu, Z.; Chen, X.; Kim, H. N.; Yoon, J. Sensors for the optical detection of cyanide ion. *Chem. Soc. Rev.* **2010**, *39*, 127−137.
(15) Li, X.; Gao, X.; Shi, W.; Ma, H. Design strategies for water-soluble small molecular chromogenic and fluorogenic probes. *Chem. Rev.* **2014**, *114*, 590−659.
(16) Lee, M. H.; Kim, J. S.; Sessler, J. L. Small molecule-based ratiometric fluorescence probes for cations anions, and biomolecules. *Chem. Soc. Rev.* **2015**, *44*, 4185−4191.
(17) Zeng, Q.; Cai, P.; Li, Z.; Qin, J.; Tang, B. Z. An imidazole-functionalized polyacetylene: Convenient synthesis and selective hemosensor for metal ions and cyanide. *Chem. Commun.* **2008**, *9*, 1094−1096.
(18) Chung, Y.; Ahn, K. H. N-acyl triazenes as tunable and selective hemodosimeters toward cyanide ion. *J. Org. Chem.* **2006**, *71*, 9470−9474.
(19) Miyaji, H.; Sessler, J. L. Off-the-shelf colorimetric anion sensors. *Angew. Chem., Int. Ed.* **2001**, *113*, 158−161.
(20) Sun, S.-S.; Lees, A. J. Anion recognition through hydrogen bonding: a simple, yet highly sensitive, luminescent metal-complex receptor. *Chem. Commun.* **2000**, *17*, 1687−1688.
(21) Anzenbacher, P.; Tyson, D. S.; Jursíková, K.; Castellano, F. N. Luminescence lifetime-based sensor for cyanide and related anions. *J. Am. Chem. Soc.* **2002**, *124*, 6232.
(22) Gimeno, N.; Li, X.; Durrant, J. R.; Vilar, R. Cyanide sensing with organic dyes: Studies in solution and on nanostructured Al2O3 surfaces. *Chem.—Eur. J.* **2008**, *14*, 3006−3012.
(23) Hawthorne, M. F.; Hammond, G. S.; Graybill, B. M. The nucleophilicity of the cyanide ion. *J. Am. Chem. Soc.* **1955**, *77*, 486−488.
(24) Zou, Q.; Tao, F.; Xu, Z.; Ding, Y.; Tian, Y.; Cui, Y. A new dibenzothiophene-based dual-channel chemosensor for cyanide with aggregation induced emission. *Anal. Methods* **2019**, *11*, 5553−5561.
(25) Zou, Q.; Tao, F.; Wu, H.; Yu, W. W.; Li, T.; Cui, Y. A new carbazole-based colorimetric and fluorescent sensor with aggregation induced emission for detection of cyanide anion. *Dyes Pigm.* **2019**, *164*, 165−173.
(26) Lee, K.-S.; Kim, H.-J.; Kim, G.-H.; Shin, I.; Hong, J.-I. Fluorescent chemodosimeter for selective detection of cyanide in water. *Org. Lett.* **2008**, *10*, 49−51.
(27) Tomasulo, M.; Sortino, S.; White, A. J. P.; Raymo, F. M. Chromogenic oxazines for cyanide detection. *J. Org. Chem.* **2006**, *71*, 744−753.
(28) García, F.; García, J. M.; García-Acosta, B.; Martínez-Máñez, R.; Sancenón, F.; Soto, J. Pyrylium containing polymers as sensoruy materials for the colorimetric sensing of cyanide in water. *Chem. Commun.* **2005**, *22*, 2790−2792.
(29) Chung, Y.; Ahn, K. H. N-acyl triazines as tunable and selective chemodosimeters toward cyanide ion. *J. Org. Chem.* **2006**, *71*, 9470−9474.
(30) Yang, Y.-K.; Tae, J. Acridinium salt based fluorescent and colorimetric chemosensor for the detection of cyanide in water. *Org. Lett.* **2006**, *8*, 5721−5723.
(31) Ros-Lis, J. V.; Martínez-Máñez, R.; Soto, J. A selective chromogenic reagent for cyanide determination. *Chem. Commun.* **2002**, *19*, 2248−2249.
(32) Kim, Y. K.; Lee, Y.-H.; Lee, H.-Y.; Kim, M. K.; Cha, G. S.; Ahn, K. H. Molecular recognition of anions through hydrogen bonding stabilization of anion-ionophore adducts: A novel trifluoroacetophenone-based binding motif. *Org. Lett.* **2003**, *5*, 4003−4006.
(33) Sun, Y.; Liu, Y.; Chen, M.; Guo, W. A novel fluorescent and chromogenic probe for cyanide detection in water based on the nucleophilic addition of cyanide to imine group. *Talanta* **2009**, *80*, 996−1000.
(34) Peng, L.; Wang, M.; Zhang, G.; Zhang, D.; Zhu, D. A fluorescent turn-on detection of cyanide in aqueous solution based on the aggregation-induced emission. *Org. Lett.* **2009**, *11*, 1943−1946.
(35) Zeler, F. H.; Männel-Croisé, C. Recent advances in the colorimetric detection of cyanide. *CHIMIA Int. J. Chem.* **2009**, *63*, 58−62.
(36) Wang, F.; Wang, L.; Chen, X.; Yoon, J. Recent progress in the development of fluorometric and colorimetric chemosensors for detection of cyanide ions. *Chem. Soc. Rev.* **2014**, *43*, 4312−4324.
(37) Pati, P. B. Organic chemodosimeter for cyanide: A nucleophilic approach. *Sens. Actuators, B* **2016**, *222*, 374−390.
(38) Padghan, S. D.; Wang, C.-Y.; Liu, W.-C.; Sun, S.-S.; Liu, K.-M.; Chen, K.-Y. A naphthalene-based colorimetric and fluorometric dual-channel chemodosimeter for sensing cyanide in a wide pH range. *Dyes Pigm.* **2020**, *183*, 108724.
(39) Luo, J.; Xie, Z.; Lam, J. W. Y.; Cheng, L.; Tang, B. Z.; Chen, H.; Qiu, C.; Kwok, H. S.; Zhan, X.; Liu, Y.; Zhu, D. Aggregation-induced emission of 1-methyl-1,2,3,4,5-pentaphenylsilole. *Chem. Commun.* **2001**, 1740−1741.
(40) Hong, Y.; Lam, J. W. Y.; Tang, B. Z. Aggregation-induced emission. *Chem. Soc. Rev.* **2011**, *40*, 5361−5538.
(41) Zhang, Y.; Li, D.; Li, Y.; Yu, J. Solvatochromic AIE luminogens as supersensitive water detectors in organic solvents and highly efficient cyanide chemosensors in water. *Chem. Sci.* **2014**, *5*, 2710−2716.
(42) Deng, K.; Wang, L.; Xia, Q.; Liu, R.; Qu, J. A turn-on fluorescent chemosensor based on aggregation-induced emission for cyanide detection and its bioimaging applications. *Sens. Actuators, B* **2019**, *296*, 126645.
(43) Gao, M.; Tang, B. Z. Fluorescent Sensors Based on Aggregation-Induced Emission: Recent Advances and Perspectives. *ACS Sens.* **2017**, *2*, 1382−1399.
(44) Huang, X.; Gu, X.; Zhang, G.; Zhang, D. A highly selective fluorescence turn-on detection of cyanide based on the aggregation of tetraphenylethylene molecules induced by chemical reaction. *Chem. Commun.* **2012**, *48*, 12195−12197.
(45) Benesi, H. A.; Hildebrand, J. H. A spectroscopic investigation of the interaction of iodine with aromatic hydrocarbons. *J. Am. Chem. Soc.* **1949**, *71*, 2703−2707.
(46) Frisch, M. J.; Trucks, G. W.; Schlegel, H. B.; Scuseria, G. E.; Robb, M. A.; Cheeseman, J. R.; Scalmani, G.; Barone, V.; Mennucci, B.; Petersson, G. A.; Nakatsuji, H.; Caricato, M.; Li, X.; Hratchian, H. P.; Izmaylov, A. F.; Bloino, J.; Zheng, G.; Sonnenberg, J. L.; Hada, M.; Ehara, M.; Toyota, K.; Fukuda, R.; Hasegawa, J.; Ishida, M.; Nakajima, T.; Honda, Y.; Kitao, O.; Nakai, H.; Vreven, T.;

https://doi.org/10.1021/acsomega.0c06080
ACS Omega 2021, 6, 16704−16713

Montgomery, J. A., Jr., Peralta, J. E.; Ogliaro, F.; Bearpark, M.; Heyd, J. J.; Brothers, E.; Kudin, K. N.; Staroverov, V. N.; Keith, T.; Kobayashi, R.; Normand, J.; Raghavachari, K.; Rendell, A.; Burant, J. C.; Iyengar, S. S.; Tomasi, J.; Cossi, M.; Rega, N.; Millam, J. M.; Klene, M.; Knox, J. E.; Cross, J. B.; Bakken, V.; Adamo, C.; Jaramillo, J.; Gomperts, R.; Stratmann, R. E.; Yazyev, O.; Austin, A. J.; Cammi, R.; Pomelli, C.; Ochterski, J. W.; Martin, R. L.; Morokuma, K.; Zakrzewski, V. G.; Voth, G. A.; Salvador, P.; Dannenberg, J. J.; Dapprich, S.; Daniels, A. D.; Farkas, O.; Foresman, J. B.; Ortiz, J. V.; Cioslowski, J.; Fox, D. J. *Gaussian 09*, Revision C.01; Gaussian, Inc.: Wallingford CT, 2010.

(47) Avogadro: an Open-Source Molecular Builder and Visualization Tool. version 1.1.0, 2016 http://avogadro.openmolecules.net/.

(48) Hanwell, M. D.; Curtis, D. E.; Lonie, D. C.; Vandermeersch, T.; Zurek, E.; Hutchison, G. R. Avogadro: An advanced semantic chemical editor, visualization, and analysis platform. *J. Cheminf.* **2012**, *4*, 17.

(49) O'Boyle, N. M.; Tenderholt, A. L.; Langner, K. M. cclib: a library for package-independent computational chemistry algorithms. *J. Comput. Chem.* **2008**, *29*, 839−845.

(50) Bolarinwa, I. F.; Oke, M. O.; Olaniyan, S. A.; Ajala, A. S. A Review of Cyanogenic Glycosides in Edible Plants. *Toxicology—New Aspects to This Scientific Conundrum*; Intechopen, 2016.

(51) Kumari, N.; Jha, S.; Bhattacharya, S. An efficient probe for rapid detection of cyanide in water at parts per billion levels and naked-eye detection of endogenous cyanide. *Chem.—Asian J.* **2014**, *9*, 830−837.

(52) Long, L.; Yuan, X.; Cao, S.; Han, Y.; Liu, W.; Chen, Q.; Han, Z.; Wang, K. Determination of Cyanide in Water and Food Samples Using an Efficient Naphthalene-Based Ratiometric Fluorescent Probe. *ACS Omega* **2019**, *4*, 10784−10790.

(53) Paquin, F.; Rivnay, J.; Salleo, A.; Stingelin, N.; Silva-Acuña, C. Multi-phase semicrystalline microstructures drive exciton dissociation in neat plastic semiconductors. *J. Mater. Chem. C* **2015**, *3*, 10715−10722.

(54) Rananaware, A.; Bhosale, R. S.; Ohkubo, K.; Patil, H.; Jones, L. A.; Jackson, S. L.; Fukuzumi, S.; Bhosale, S. V.; Bhosale, S. V. Tetraphenylethene-Based Star Shaped Porphyrins: Synthesis, Self-Assembly, and Optical and Photophysical Study. *J. Org. Chem.* **2015**, *80*, 3832−3840.

(55) Li, J.; Wang, J.; Li, H.; Song, N.; Wang, D.; Tang, B. Z. Supramolecular materials based on AIE luminogens (AIEgens): construction and applications. *Chem. Soc. Rev.* **2020**, *49*, 1144−1172.

(56) Manickam, S.; Iyer, S. K. Highly Sensitive Turn-off Fluorescent Detection of Cyanide in Aqueous Medium Using Dicyanovinyl-Substituted Phenanthridine Fluorophore. *RSC Adv.* **2020**, *10*, 11791−11799.

https://doi.org/10.1021/acsomega.0c06080
ACS Omega 2021, 6, 16704−16713